

Technical Report Documentation Page

1. Report No. TX -97/0-1704-4R	2. Government Accession No.	3. Recipient's Catalog No.	
4. Title and Subtitle Visibility Calculation from Video Images Using Different Techniques		5. Report Date January 1998	
		6. Performing Organization Code TECH	
7. Author(s) Douglas D. Gransberg, Sanjaya Senadheera, Olkan Culvalci, Bobby Green, Alexandr Gilman, and Joe Alvarez		8. Performing Organization Report No. Interim Research Report 1704-4R	
9. Performing Organization Name and Address Texas Tech University Departments of Engineering Technology and Mechancial Engineering Box 43107 Lubbock, Texas 79409-3107		10. Work Unit No. (TRAIS)	
		11. Contract or Grant No. Project 0-1704-4	
12. Sponsoring Agency Name and Address Texas Department of Transportation Research and Technology P. O. Box 5080 Austin, TX 78763-5080		13. Type of Report and Period Cover Interim Research April 1997-August 1997	
		14. Sponsoring Agency Code	
15. Supplementary Notes Study conducted in cooperation with the Texas Department of Transportation. Research Project Title: "Evaluation of Roadway Lighting Systems Designed by STV Methods"			
16. Abstract Four different calculation methods were performed to determine the contrast of an STV target between illuminance assemblies mounted on poles: STV (small target visibility), STV with n points, STV by comparing the areas, and STV by patching. These experiments were performed under the original site conditions and after all the luminaire heads were replaced with new 250 Watt luminaires. The original conditions consisted of a combination of 250 Watt and 400 Watt lamps. Before replacing the luminaire heads, the target had 40% contrast. After replacing the luminaires with the 250 Watt luminaire heads, contrast increased to 85%. STV by patching was the least preferred method, and STV by comparing the areas was the second least preferred method for contrast calculation. STV was a poor method to calculate the contrast because of the small number of data points used for calculation.			
17. Key Words Small Target Visibility, Roadway Lighting, Luminaire		18. Distribution Statement No restrictions. This document is available to the public through the National Technical Information Service, Springfield, Virginia 22161	
19. Security Classif. (of this report) Unclassified	20. Security Classif. (of this page) Unclassified	21. No. of Pages 35	22. Price

Implementation Statement

At this point in time, experimental work has not been completed to validate the inferences made in this report. However, the trends evident the experimental work completed to date seems to indeed support the conclusions. Therefore a recommendation is tentatively made that the Texas Department of Transportation choose not to implement Small Target Visibility (STV) design methodology even if it is adopted as a National standard for roadway lighting design.

Dissemination of this information will best be accomplished through the Traffic Operations Division. A letter clearly stating the policy for roadway lighting design should be published and disseminated to all districts.

Disclaimer

The contents of this report reflect the views of the authors, who are solely responsible for the facts and the accuracy of the data presented herein. The contents do not necessarily reflect the official view or policies of the Texas Department of Transportation. This report does not constitute a standard, specification, or regulation.

Acknowledgements

The authors would like to take this opportunity to acknowledge the valuable contributions of the following people:

Karl Burkett, P.E., Project Director, Traffic Operations Division, TxDOT
Dr. Werner Adrian, McGill University, Waterloo, Canada

Table of Contents

Implementation Statement	i
Disclaimer	i
Acknowledgements	i
Table of Contents	ii
List of Figures	ii
List of Tables	iv
Abstract	1
Introduction	1
Experimental Field and Target	3
Video Camera	6
Contrast Analysis	7
Results and Discussion	10
Original Luminaire Head	10
Analysis with Standard Fixture	17
Conclusions	29
Bibliography	30

List of Figures

Figure 1	Measurements of the Experiment Field	4
Figure 2	Experiment Set-Up	5
Figure 3	Target Front View and Side View	5
Figure 4	Contrast Analysis for the Target	7

Figure 5	Contrast between Poles 9A and 10A on the West and East Lines Under the Original Conditions Using the STV Method	11
Figure 6	Contrast between Poles 9A and 10A on the West and East Lines Under the Original Conditions Using the STV with n Points Method	11
Figure 7	Contrast Comparison between Poles 9A and 10A on the West and East Lines Under Original Conditions Using the STV and STV with n Points Methods	12
Figure 8	Contrast between Poles 9A and 10A on the West and East Lines Under Original Conditions Using the STV by Comparing the Areas Method	12
Figure 9	Contrast between Poles 9A and 10A on the West and East Lines Under Original Conditions Using the STV by Patching Method	13
Figure 10	Contrast between Poles 10A and 11A on the West and East Lines Under Original Conditions Using the STV Method	14
Figure 11	Contrast between Poles 10A and 11A on the West and East Lines Under Original Conditions Using the STV with n Points Method	15
Figure 12	Contrast Comparison between Poles 10A and 11A on the West and East Lines Under Original Conditions Using the STV and STV with n Points Methods	15
Figure 13	Contrast between Poles 10A and 11A on the West and East Lines Under Original Conditions Using the STV by Comparing the Areas Method	16
Figure 14	Contrast between Poles 10A and 11A on the West and East Lines Under Original Conditions Using the STV by Patching Method	16
Figure 15	Contrast between Poles 9A and 10A on the West and East Lines Under the Replaced 250 Watt Luminaire Heads Using the STV Method	17
Figure 16	Contrast between Poles 9A and 10A on the West and East Lines Under the Replaced 250 Watt Luminaire Heads Using the STV with n Points Method	17
Figure 17	Contrast Comparison between Poles 9A and 10A on the West and East Lines Under the Replaced 250 Watt Luminaire Heads Using the STV And STV with n Points Methods	18

Figure 18	Contrast between Poles 9A and 10A on the West and East Lines Under the Replaced 250 Watt Luminaire Heads Using the STV by Comparison the Areas Method	18
Figure 19	Contrast between Poles 9A and 10A on the West and East Lines Under the Replaced 250 Watt Luminaire Heads Using the STV by Patching Method	19
Figure 20	Contrast between Poles 10A and 11A on the West and East Lines Under the Replaced 250 Watt Luminaire Heads Using the STV Method	19
Figure 21	Contrast between Poles 10A and 11A on the West and East Lines Under the Replaced 250 Watt Luminaire Heads Using the STV with <i>n</i> Points Method	20
Figure 22	Contrast Comparison between Poles 10A and 11A on the West and East Lines Under the Replaced 250 Watt Luminaire Heads Using the STV and STV with <i>n</i> Points Methods	20
Figure 23	Contrast between Poles 10A and 11A on the West and East Lines Under the Replaced 250 Watt Luminaire Heads Using the STV by Comparing the Areas Method	21
Figure 24	Contrast between Poles 10A and 11A on the West and East Lines Under the Replaced 250 Watt Luminaire Heads Using the STV by Patching Method	21
Figure 25	Contrast Comparison between Poles 9A and 10A on the West and East Lines Under the Original Conditions Using the STV, STV with <i>n</i> Points, STV by Comparing the Areas, and STV by Patching Methods	22
Figure 26	Contrast Comparison between Poles 9A and 10A on the West and East Lines Under the Replaced 250 Watt Luminaire Heads Using the STV, STV with <i>n</i> Points, STV by Comparing the Areas, and STV by Patching Methods	23
Figure 27	Video Image at the First Location	24
Figure 28	Video Image at the Second Location	24
Figure 29	Video Image at the Third Location	25
Figure 30	Video Image at the Fourth Location	25
Figure 31	Video Image at the Fifth Location	26

Figure 32	Video Image at the Sixth Location	26
Figure 33	Video Image at the Seventh Location	27
Figure 34	Video Image at the Eighth Location	27
Figure 35	Video Image at the Ninth Location	28
Figure 36	Video Image at the Tenth Location	28

List of Tables

Table 1	Original and Replacement Luminaires	10
---------	-------------------------------------	----

Visibility Calculation from Video Images Using Different Techniques

Abstract

Four different calculation methods were performed to determine the contrast of an STV target between illuminance assemblies mounted on poles: STV (small target visibility), STV with n points, STV by comparing the areas, and STV by patching. These experiments were performed under the original site conditions and after all the luminaire heads were replaced with new 250 Watt luminaires. The original conditions consisted of a combination of 250 Watt and 400 Watt lamps. Before replacing the luminaire heads, the target had 40% contrast. After replacing the luminaires with the 250 Watt luminaire heads, contrast increased to 85%. STV by patching was the least preferred method, and STV by comparing the areas was the second least preferred method for contrast calculation. STV was a poor method to calculate the contrast because of the small number of data points used for calculation.

Introduction

The traditional goniometer technique (a single intensity reading such as luminance/illuminance is collected in sequence) is well known. Many authors have completed experimental studies for roadway lighting design using the goniometer technique.

Rackoff and Rackwell (1975) developed a vehicle-based television system to investigate driving vision patterns during nighttime driving. The system compared vision patterns during nighttime driving to vision patterns during daytime driving on freeways and a rural highway. The system also determined differences in vision patterns at sites with high and low nighttime accident rates and the effect of illuminance on a driver's vision pattern. The researchers found nighttime vision patterns were different from daytime vision patterns. The changes in vision patterns due to the amount of illuminance prove that illuminance can affect a driver's ability to see effectively.

Janoff et al. (1986) tried to determine if roadway lighting can be reduced or eliminated at night when traffic volume is much lower than design capacity without significantly reducing drivers' abilities to control their vehicles safely and effectively. Researchers used a Styrofoam hemisphere with a 6-in (0.15-m) diameter skirt with an 18% reflecting surface. The research team obtained a linear relation between the detection distance and horizontal illuminance and the pavement luminance and contrast index by using six different lighting methods as parameters:

every luminaire lit, 75 % of the luminaires lit, 50% of the luminaires lit, every other luminaire lit, luminaires on only one side of the road lit, and no luminaires lit. Results of the controlled field experiments show that drivers felt more negative toward reducing the lighting on all ramps and interchanges than the lighting on straight mainline roadway sections.

Zwahlen and Yu (1990) performed two investigations to determine the distances at which the color and shape of a target can be identified at night under vehicle low-beam illuminance. The targets were flat and one of three shapes and one of six colors. First, distances for color and shape recognition were investigated. Second, distance for color recognition only was investigated. The target colors were red, green, yellow, orange, blue or white. The target shapes were a circle, square or diamond and had a surface area of 36 in². Results of the investigations show that the distance for color recognition was twice as far as the distance for shape recognition. Researchers found the saturated red retroreflective targets to be most visual of all the target colors.

Hall and Fisher (1978) examined the design of a roadway lighting system by using empirically derived requirements of light technical parameters such as road luminance, luminance uniformity, and glare restriction. The researchers used a square target (200 mm x 200 mm) with a limited range of contrast. They found that lighting design based on a contrast matrix yields good results.

Marsden (1976) studied road lighting contrast and accident reduction, both numerically and experimentally. During the experimental investigation the disability glare was related to veiling luminance, measured with a Pritchard photometer. Horizontal illuminance near the road surface was measured by summing the outputs of photocells mounted on each end of the vehicle. Vertical illuminance near the road surface was measured by a photocell mounted on the rear of the vehicle. Some instrumentation was also mounted below the vehicle to record road reflectance data. Researchers recorded all this information and the visual field of the driver with a video recorder. The video was played in the laboratory and could be frozen on a selected frame. Certain areas on the frame could be defined (by operating brightening-up controls) for luminance analysis. This analysis was examined on the portion of the TV signal corresponding to the selected area. Analog processing gave the value of maximum, minimum, average and standard deviation of luminance within the selected area by using a calibration luminance scale.

In previous studies researchers used humans to detect the distance at which shape, color and contrast are recognized. Experimental results fluctuated because every human eye detects shapes

and colors at different distances. Additional information at the site of the experiment such as weather conditions and sensitivity of the experiment equipment effected the results. One of the most important issues for experimental research is eliminating those site effects as much as possible.

In this study a 3-CCD video camera was used instead of a human eye. The 3-CCD camera was mounted 83 m away from and 1.62 m above an 18 cm x 18 cm, 20% reflective target. The target was located in the middle of the camera frame and satisfied the 1 degree angle (STV requirement) as seen in Figure 2. All information (global information) was recorded on a video camera. The video was played in the laboratory and selected frames, including the target, could be frozen and loaded into the computer for analysis.

Programs were developed to read and analyze photometric data from the video tape. The analyses were examined including the portion of the frame with the target. In the selected portion, a pixel analysis was performed to investigate the contrast of the STV target. These pixels included global information such as luminance, illuminance, and reflection information. Through the pixel analysis, contrast distributions were obtained between the roadway lights. Therefore, the measurement and analysis system was independent from an individual's eye response.

Experimental Field and Target

All experimental investigations were performed on a single lane road on the west side of a rest area north of Abernathy, Texas between Abernathy and Halecenter, Texas on Texas Interstate Highway 27. Figure 1 shows the dimensions and orientation for the test field.

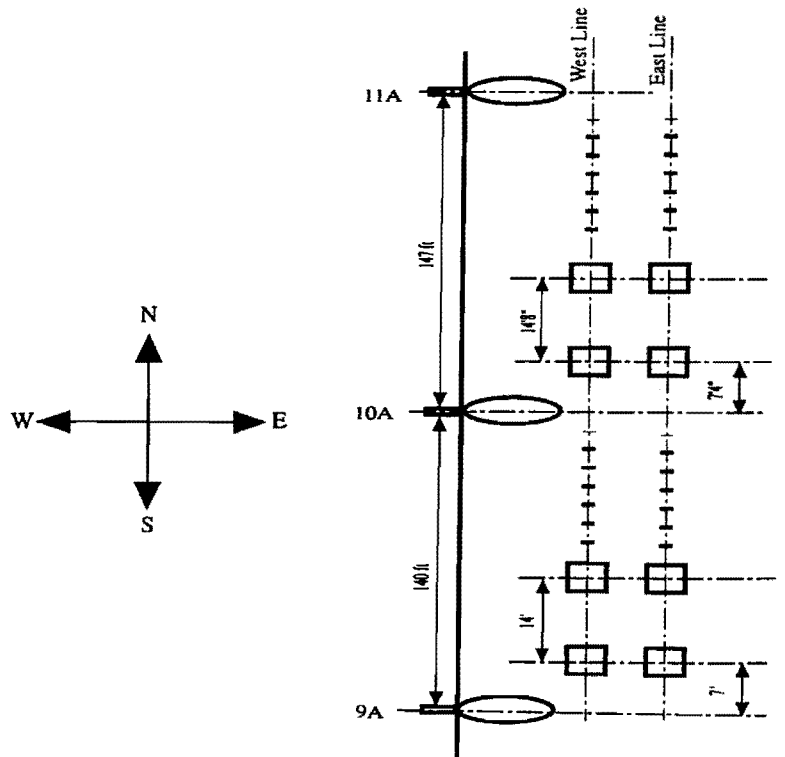
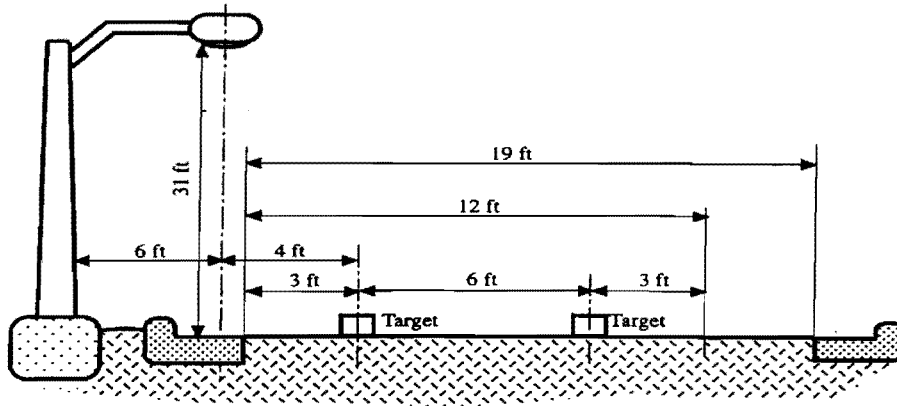


Figure 1 Measurements of the Experiment Field

The STV was used for comparison during the experiment as a static model since there was no relative motion between the camera and the target during the experiment. Distances and orientation of the camera and the target views are shown in Figures 2 and 3, respectively.

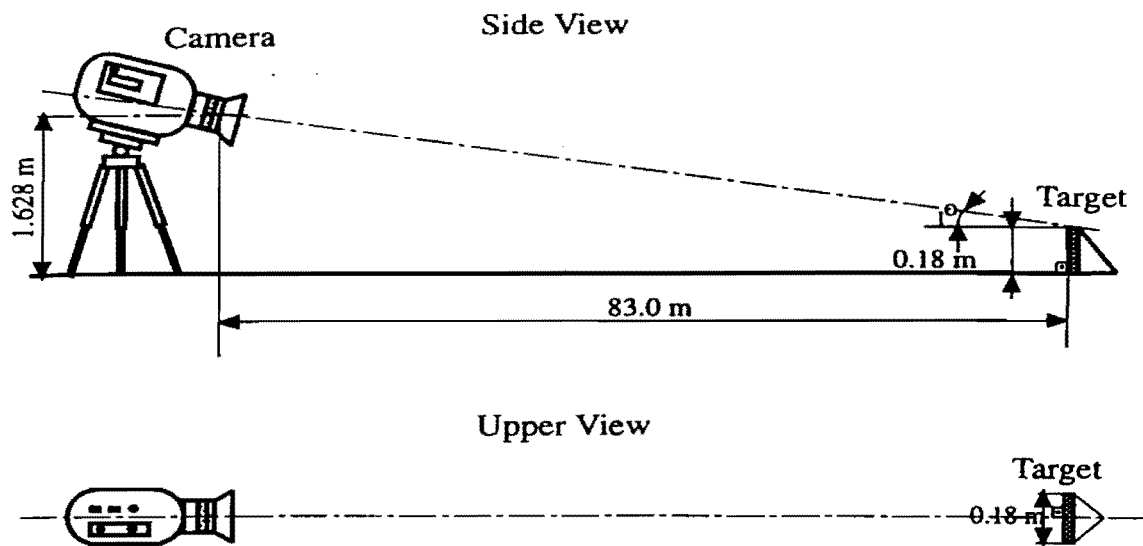


Figure 2 Experiment Set-Up

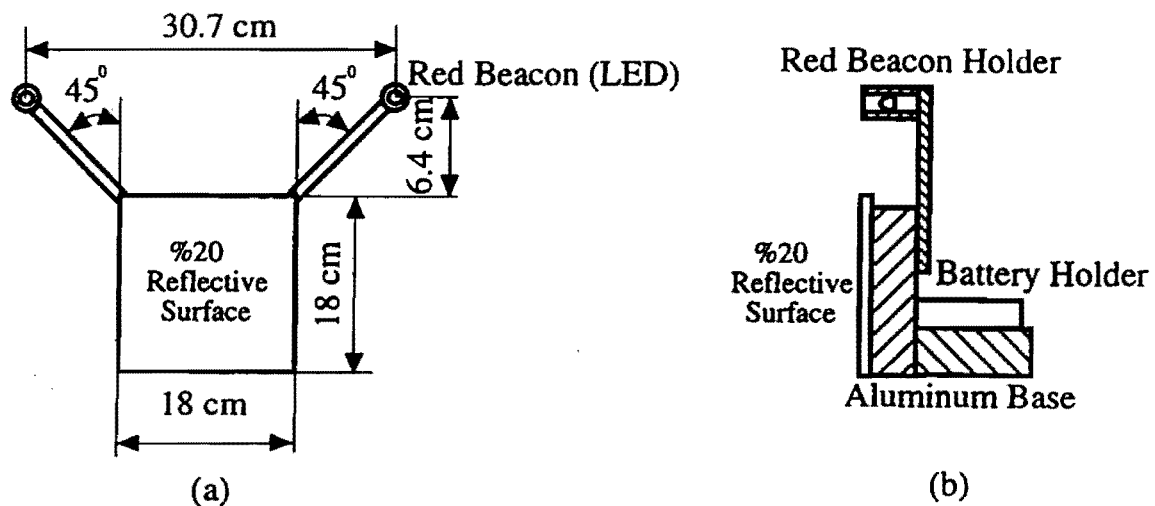


Figure 3 Target (a) Front View, (b) Side View

The STV target was built using two aluminum pieces connected together at a 90 degree angle to make the foundation and vertical plane of an STV target. Two more aluminum holders were designed to mount red LEDs at a 45 degree angle from the vertical line. An 18 x 18 cm, 20%

reflective gray scale paper was placed on the vertical surface of the aluminum frame for an STV target.

Video Camera

Using a film camera as an absolute photometry to measure entire light distributions became a very important research topic in the 1960's. But the film itself created problems like stable replacement and was an unreliable means of collecting the image due to film nonlinearities. A charged, coupled device (CCD) in a solid state video camera removed most of the problems associated with the film cameras.

The data acquisition system was built as two pieces. One was a 3-CCD analog video camera and a single CCD digital video camera, and the other was a PC computer using an analog video capture data analysis card. The 3-CCD camera system employs high density, three-chip precision. Each CCD image includes a total of about 410,000 picture elements. Some technical specifications of the 3-CCD video camera are listed below:

Video recording system Rotary two heads, helical scanning FM system

Video signal NTSC color, EIA standards

Usable cassette 8 mm video format cassette (Hi8 or standard 8 mm)

Image device 3-CCD (Each Charge Coupled Device is 1/3 sq. in)

Viewfinder Electronic viewfinder (monochrome)

Lens Combined 12 x power zoom lens $f = 5.5$ to 66 mm, F1.6 to 1.8, 40 to 480 mm when converted into a 35-mm still camera, filter diameter 52 mm, TTL autofocus system, inner focus wide macro system

Minimum illuminance 4 Lx (F1.6)

Illuminance range 4 Lx to 100,000 Lx (0.37 to 9.294 foot-candles)

A Hi8 video camera recorder should use Hi8 video cassettes for higher-quality video images. An IBM compatible computer that has a Pentium 300 MHz processor, 128MB RAM memory, a 6.0 GB hard drive, and an analog video capture card was used as a data analysis system.

Contrast Analysis

Four different methods were developed to calculate the contrast analysis: STV, STV with n points, STV by comparing the area, and STV by patching as seen in Figure 4a, 4b, 4c and 4d.

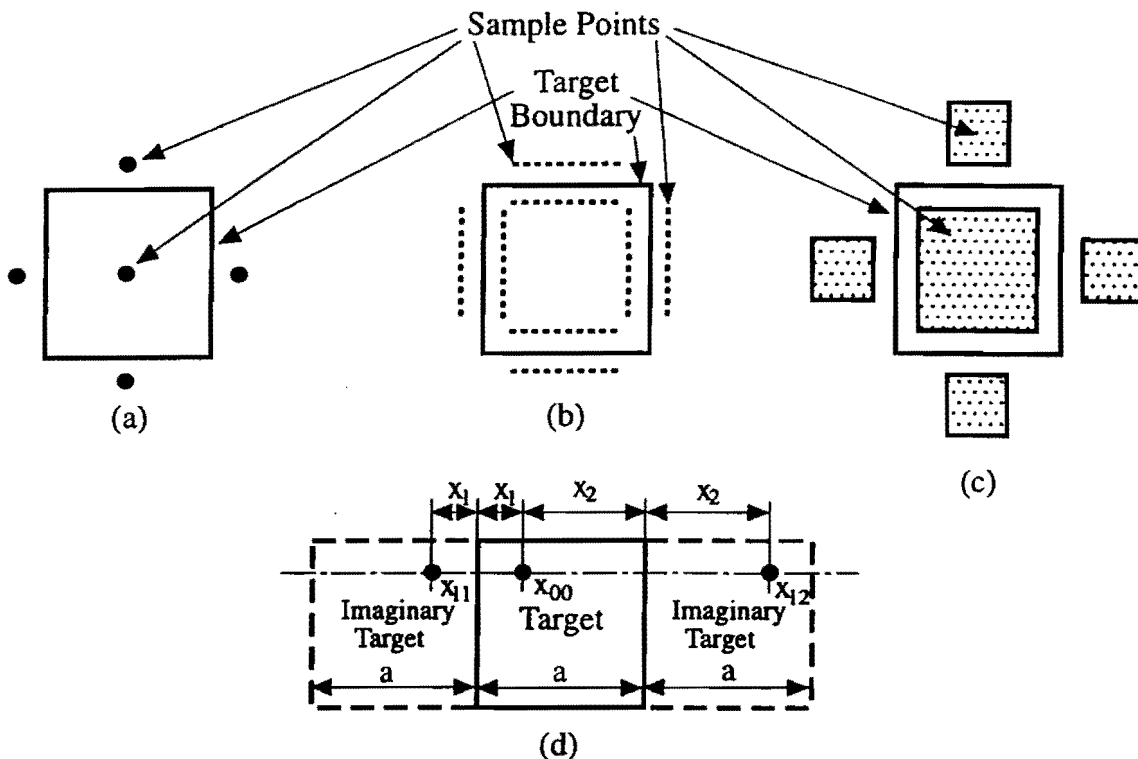


Figure 4 Contrast Analysis for the Target (a) STV, (b) STV with n Points, (c) STV by Comparing the Areas, and (d) STV by Patching Methods

First, contrast calculations were performed for the small target. One point was marked on the center of the target reflection surface. Four boundary points were marked on the square target in the x and y -direction. All four points were equal distance from the target center as seen in Figure 4a. Contrast of the target was calculated by taking the difference between the outside points and the center point. The average of the values was taken as the average contrast of the target for the STV method.

Next, several data points were recorded inside and outside the target boundary for the STV with n points method as seen in Figure 4b. The averages for the inside and outside points were

calculated separately, and the difference of these values were obtained for each boundary. The average of the values was taken as the average contrast of the target for the STV with n points method.

Then, by using central limit theory for contrast calculation, the STV by comparing areas method was performed. Central limit theory indicates that normal distribution is appropriate to calculate the approximate distribution of an average for a set of identically distributed random variables, regardless of the distribution of the individual random variables. On the other hand, it is known that if a set of independent random variables is obtained with the same distribution of mean, μ , and variance, σ^2 , the variables are always mean, μ , and variance, σ^2/n . The average of the independent random variables is normally distributed if all the individual random variables are normally distributed. Assuming actual distribution of the individual random variables, X_1, \dots, X_n , the distribution of their average, \bar{X} , is closely approximated by $N(\mu, \sigma^2/n)$ distribution. The n value should be greater than 30 for good approximation.

A square smaller than the 18cm x 18cm target was symmetrically marked on the reflective surface, and it was divided into four equal smaller squares. Four new squares, which were equal to the four equal smaller squares, were symmetrically marked outside the target boundaries as seen in Figure 4c. Therefore, the area of the square inside the target boundary was equal to the total area of the four squares outside the target. The central limit theory was applied to the problem. The number of data was observed more than 30 ($n > 30$). The variance was unknown, and the distribution was normal because of the light reflection data. The sample variance was obtained from the population with a mean, μ , and a variance, σ^2 .

$$\sigma^2 = S^2 = \frac{\sum_{i=1}^n (X_i - \bar{X})^2}{n-1}. \quad (1)$$

In Figure 4c a two-sample, t-procedure method was used by comparing the areas inside and outside the target for contrast calculation. One sample had a size n from population A with a mean x and standard deviation S_x . Another sample had a size m from population B with a mean y and standard deviation S_y . The confidence interval length depends upon the confidence level $1 - \alpha$ through the critical point. Confidence levels of 90%, 95% and 99% are typically used. These levels correspond to values of 0.10, 0.05 and 0.01, respectively. A two-sided, $1 - \alpha$ level confidence interval for the difference in population means $\mu_A - \mu_B$ is shown in the equation below.

$$\mu_A - \mu_B \in \left(\bar{x} - \bar{y} + t_{\alpha/2, v} \sqrt{\frac{S_x^2}{n} + \frac{S_y^2}{n}}, \bar{x} - \bar{y} - t_{\alpha/2, v} \sqrt{\frac{S_x^2}{n} + \frac{S_y^2}{n}} \right) \quad (2)$$

The degrees of freedom of the critical point v are calculated by using following formula.

$$v = \frac{\left(\frac{S_x^2}{n} + \frac{S_y^2}{m} \right)^2}{\frac{S_x^4}{n^2(n-1)} + \frac{S_y^4}{m^2(m-1)}}, \quad (3)$$

And $t_{\alpha/2, v}$ was obtained from the table of critical points of the t -distribution.

Next, the patch method was applied to the target to obtain contrast. For the patch method, a small portion, including the target, was selected from a frame. Two imaginary targets were added to both sides of the actual target, and in the selected portion the actual target was removed as seen in Figure 4d. The target's background was filled using neighboring pixels horizontally. Now contrast of the target was affected by dynamic variation of contrast. Therefore, a pixel, x_{00} , with coordinates x_1 and x_2 was pointed on the target surface, and the x_1 and x_2 distances were calculated as ratios according to the target length, a , such as $r_1 = 1 - x_1/a$ and $r_2 = 1 - x_2/a$, respectively. The effect of the neighboring pixels on the original point was calculated according to the ratios. For example, the pixel numbers x_{11} and x_{12} were multiplied by the ratios r_1 and r_2 , respectively. These numbers were then added together, and this new number replaced the original point x_{00} . To obtain a background image, the procedure was repeated for all the pixels until the inside of the target boundaries was filled. Then, a new image was obtained by individually creating each pixel between the target and the background image. The central limit theory was again applied to the new image to calculate contrast of the target.

Results and Discussion

Video images were recorded between the illuminance assemblies mounted on poles 9A and 10A and 10A and 11A under the original conditions found at the site (luminaire heads, lenses, and lamps were left as found). The original luminaire heads were 250 and 400 Watts and from various manufacturers. Two sets of measurements were taken, first for clean luminaire lenses then for dirty luminaire lenses, all the heads were then replaced with new General Electric luminaire heads (M400R2 Luminaire, Catalog number M4RR25S9M4GMS3072) with 250 HPS (Sylvania) lamps and measurements were taken again. Contrasts of the targets were calculated by applying the four different calculation methods to the target, and the results were studied. The individual contrast distribution of the target starts with a high value at the first location and reduces to a significantly lower value at the second location. The second location is 15% of the distance between the two poles starting from the first location. After the second location, contrast values increase until the second pole. If contrast was under 10%, the target was considered invisible. This corresponds to the threshold luminance calculation by Adrian and was verified visually by researchers in the field. Table 1 shows the conditions of the original and replaced luminaires.

Table 1 Original and Replacement Luminaires

Roadway Lighting Pole Number	8A	9A	10A	11A	12A
Original Conditions	400 Watt	250 Watt	400Watt	250 Watt	250 Watt
Original Lamp Head*	A-E	G-E	A-E	C-H	C-H
Replacement Conditions	250 Watt	250 Watt	250 Watt	250 Watt	250 Watt
Replacement Lamp Head*	G-E	G-E	G-E	G-E	G-E

*A-E American Electric, G-E General Electric, C-H Crouse-Hinds

Original Luminaire Head

Figures 5 and 6 show contrast between poles 9A and 10A under the original conditions using the methods STV and STV with n points, respectively.

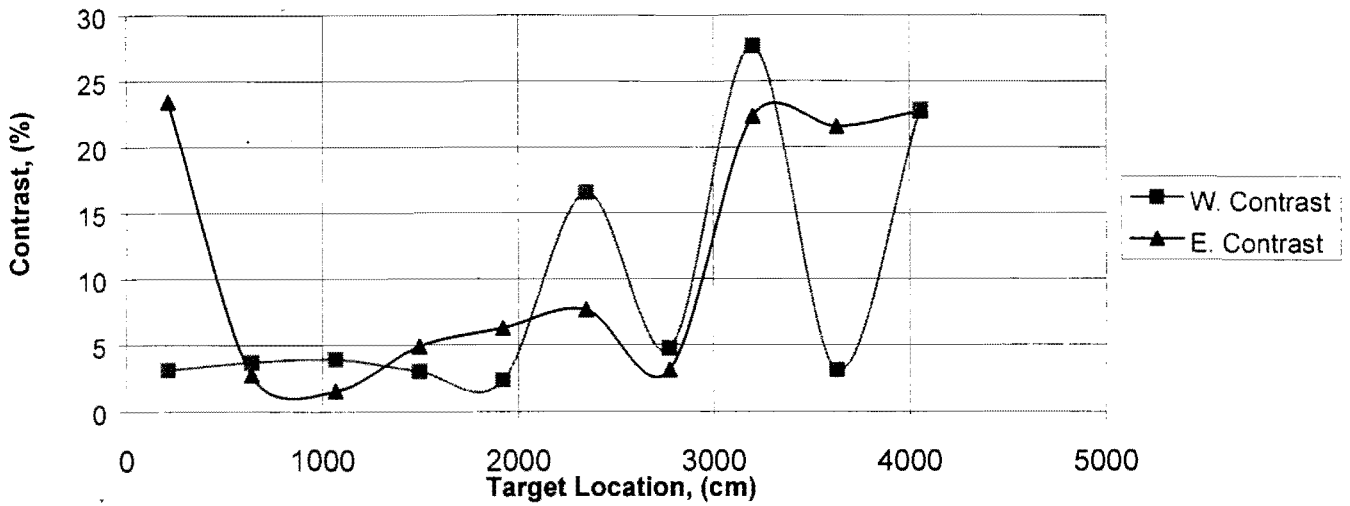


Figure 5 Contrast Between Poles 9A and 10A on the West and East Lines Under the Original Conditions Using the STV Method

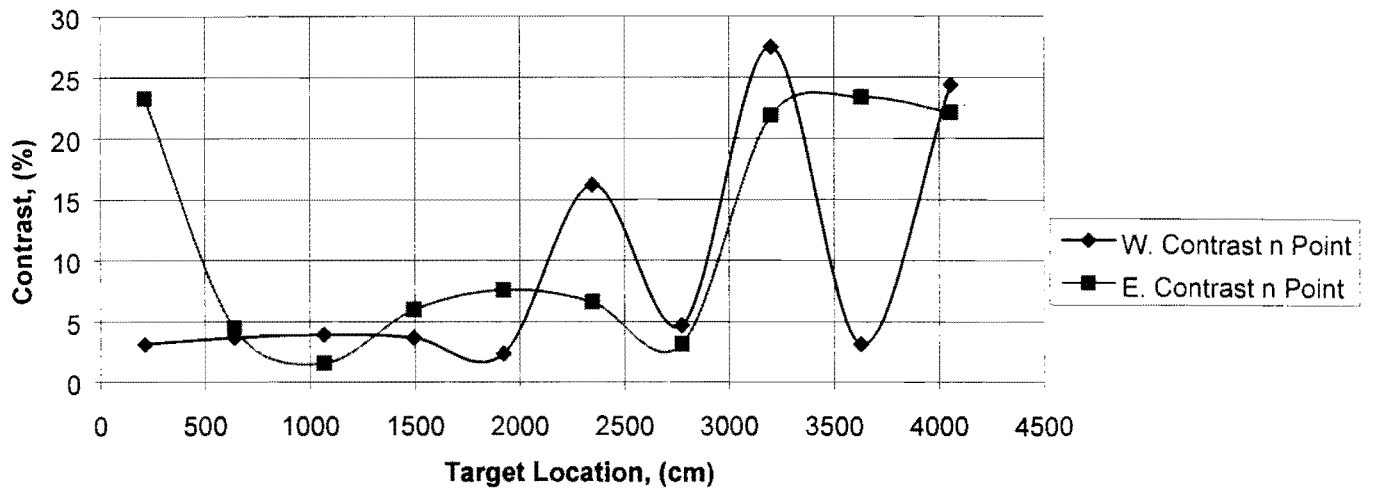


Figure 6 Contrast Between Poles 9A and 10A on the West and East Lines Under the Original Conditions Using STV with *n* Points Method

Contrast under the original conditions in the west lane shows fluctuating contrast values due to old lamps and very dirty lenses on the illuminance assemblies mounted on the poles. Figure 7 shows contrast values are slightly different between the STV and STV with *n* points methods, but the difference is not significant.

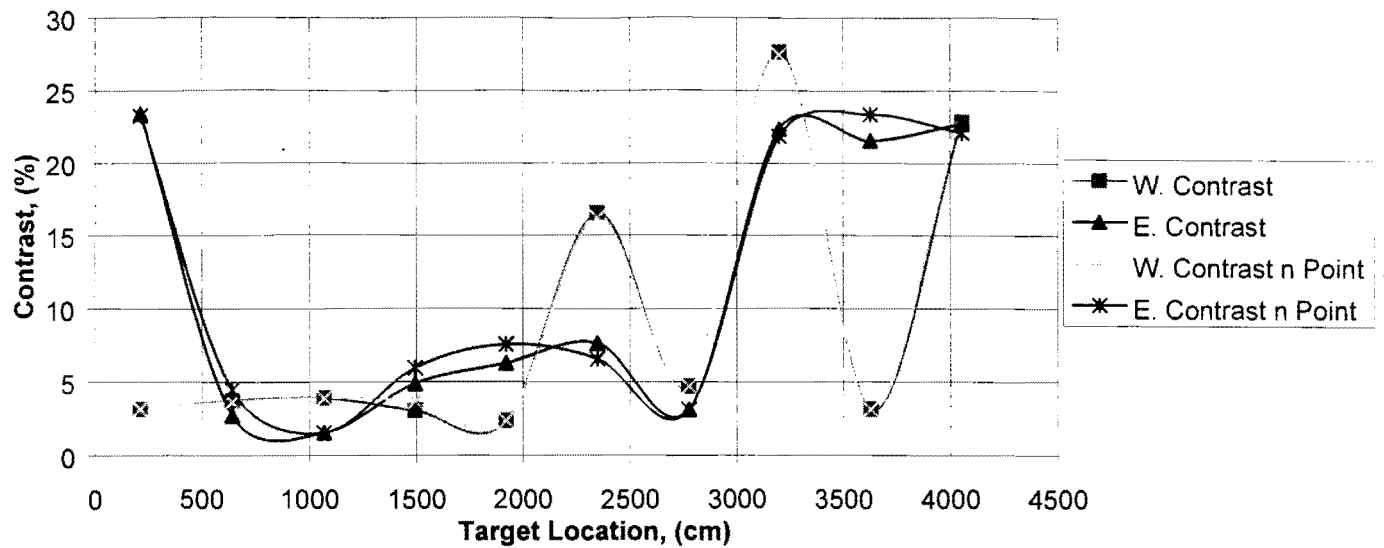


Figure 7 Contrast Comparison Between Poles 9A and 10A on the West and East Lines Under Original Conditions Using STV and STV with *n* Points Methods

The methods of STV by comparing the areas and STV by patching were applied to obtain contrast of the target as seen in Figures 8 and 9, respectively.

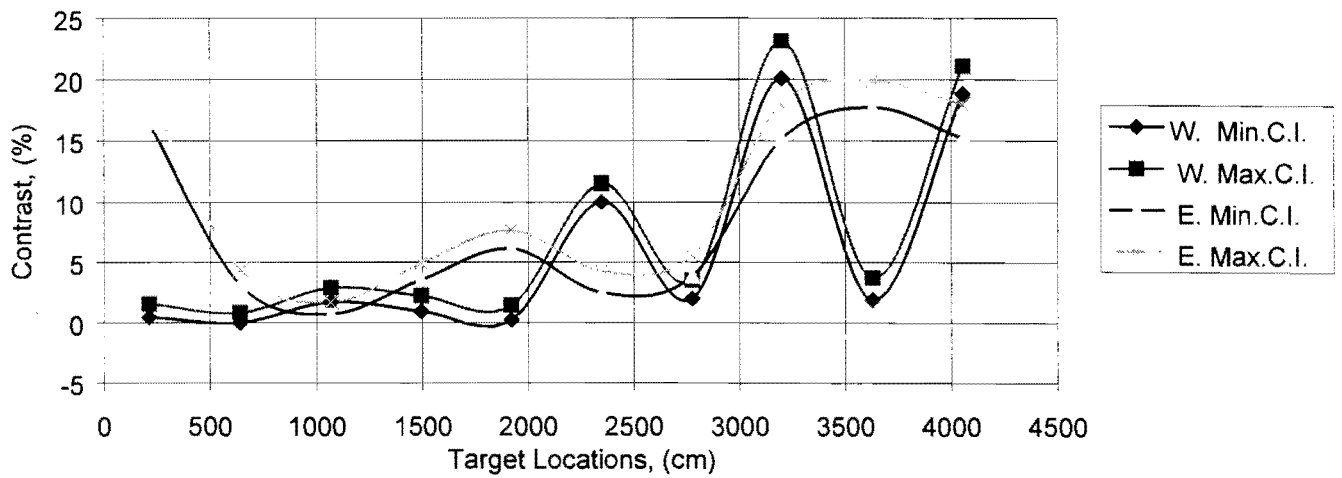


Figure 8 Contrast Between Poles 9A and 10A on the West and East Lines Under Original Conditions Using STV by Comparing the Areas Method

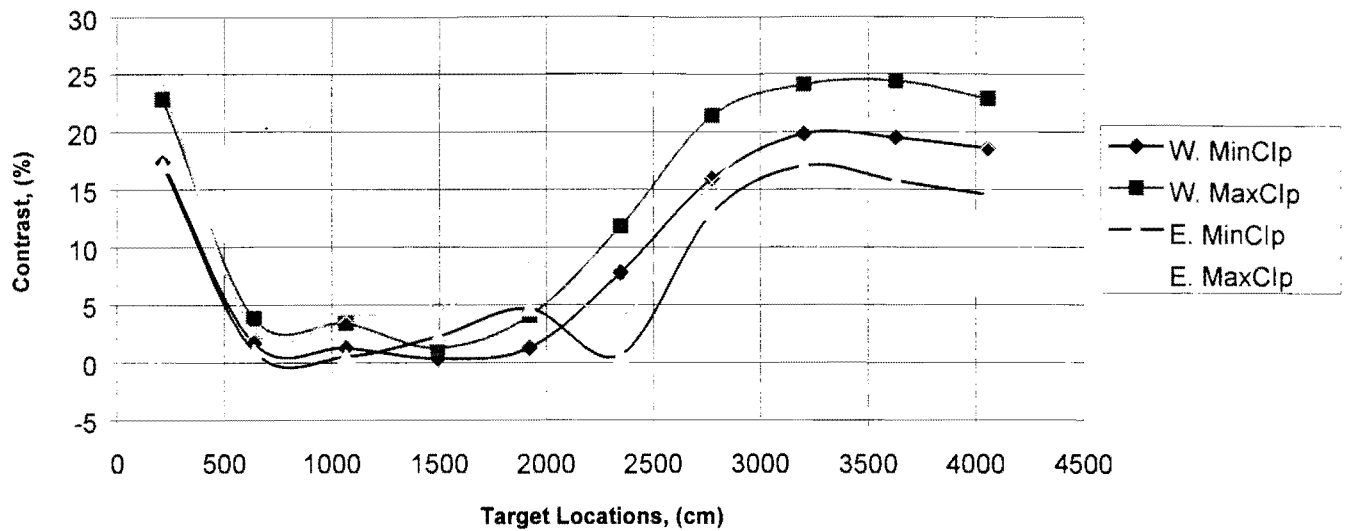


Figure 9 Contrast Between Poles 9A and 10A on the West and East Lines Under Original Conditions Using STV by Patching Method

For these methods, the maximum and minimum values of contrast were calculated using the central limit theory, assuming a 95% confidence level. The contrast values of the target lie between these values with a 95% confidence level. Figure 8 shows more detailed results than Figures 5 and 6 since more pixels were taken into account for this contrast calculation. Figure 9 has a large variation because contrast was calculated by patching the background of the target using horizontal pixel distribution.

The same experiments were performed between the illuminance assemblies mounted on poles 10A and 11A, and in Figure 10 and 11 results were plotted for the STV and STV with n points methods, respectively.

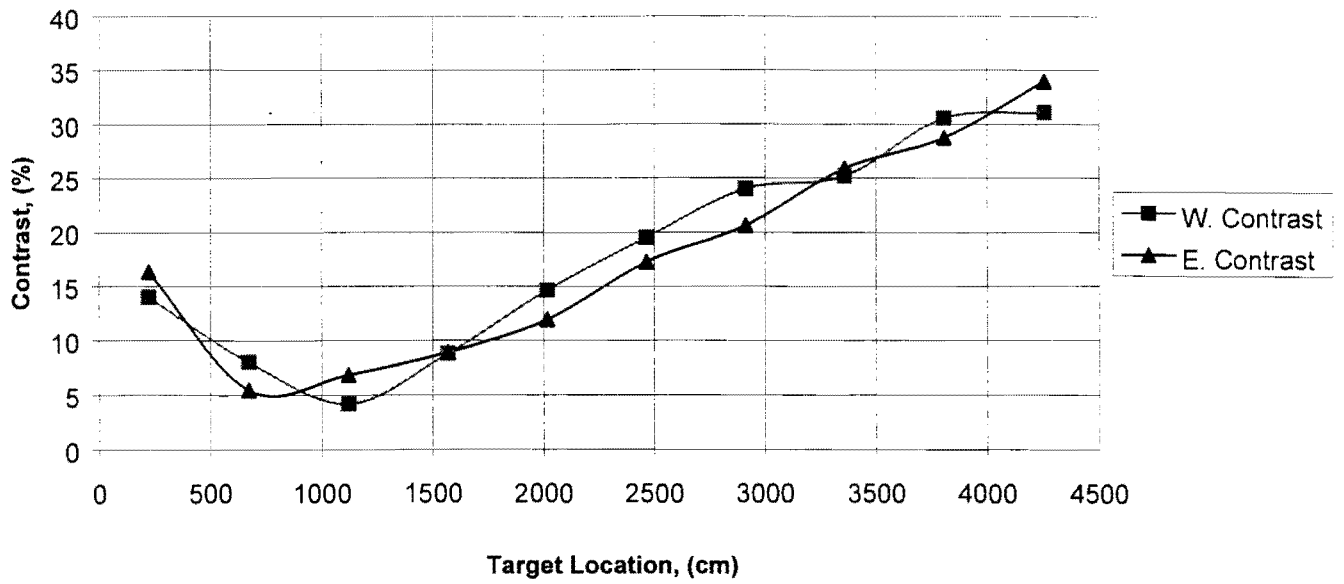


Figure 10 Contrast Between Poles 10A and 11A on the West and East Lines Under Original Conditions Using STV Method

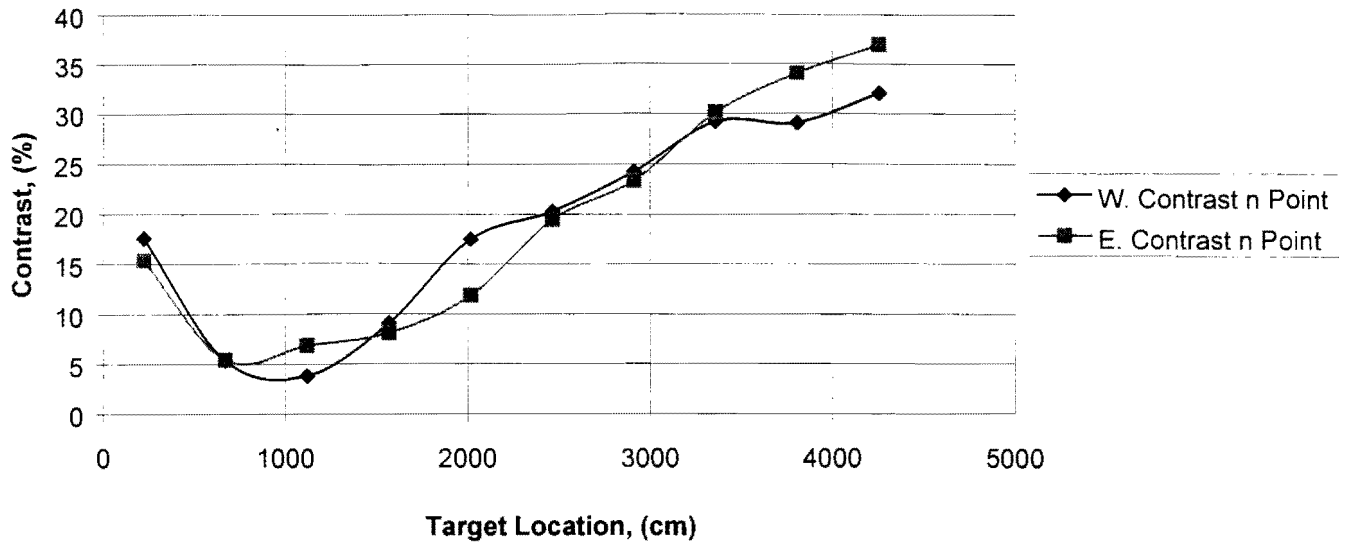


Figure 11 Contrast Between Poles 10A and 11A on the West and East Lines Under Original Conditions Using STV with n Points Method

In Figure 12, the shaded areas show the difference between the two methods for the west and east lines.

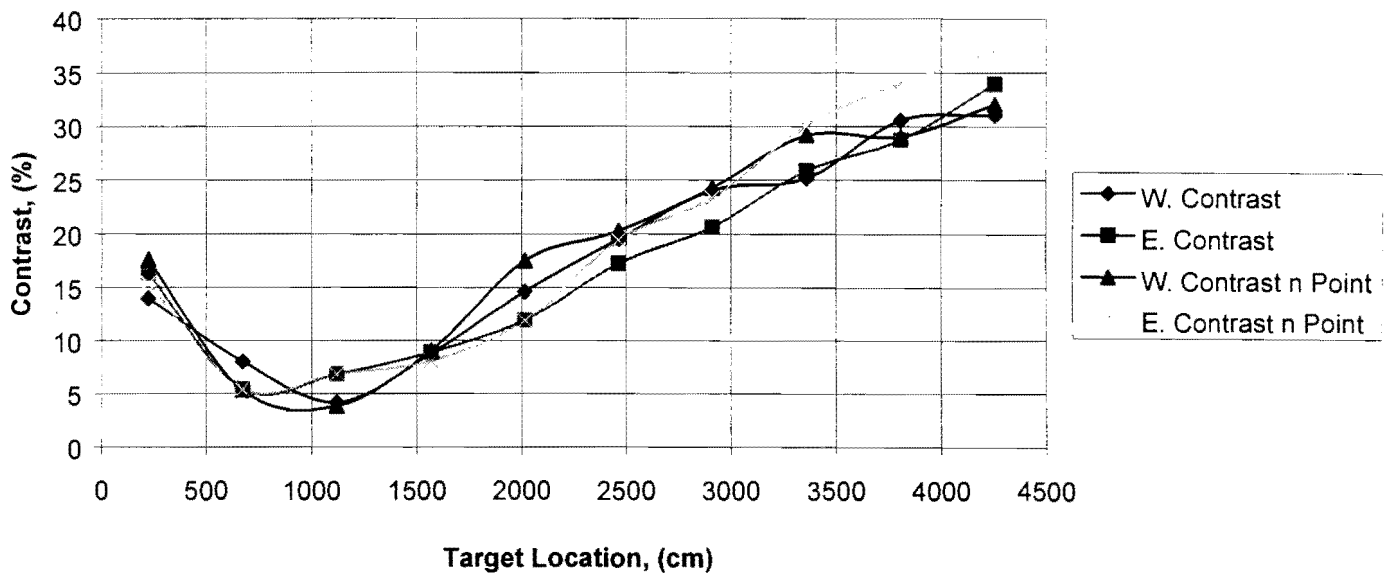


Figure 12 Contrast Comparison Between Poles 10A and 11A on the West and East Lines Under Original Conditions Using STV and STV with n Points Methods

Figures 13 and 14 show contrast distribution for STV by comparing the areas and STV by patching methods, respectively.

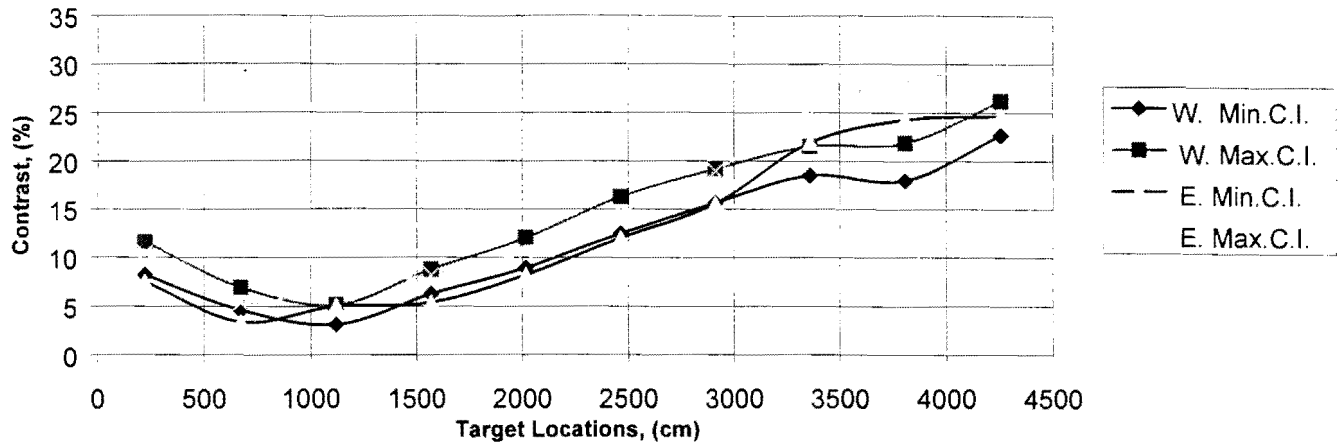


Figure 13 Contrast Between Poles 10A and 11A on the West and East Lines Under Original Conditions Using STV by Comparing the Areas Method

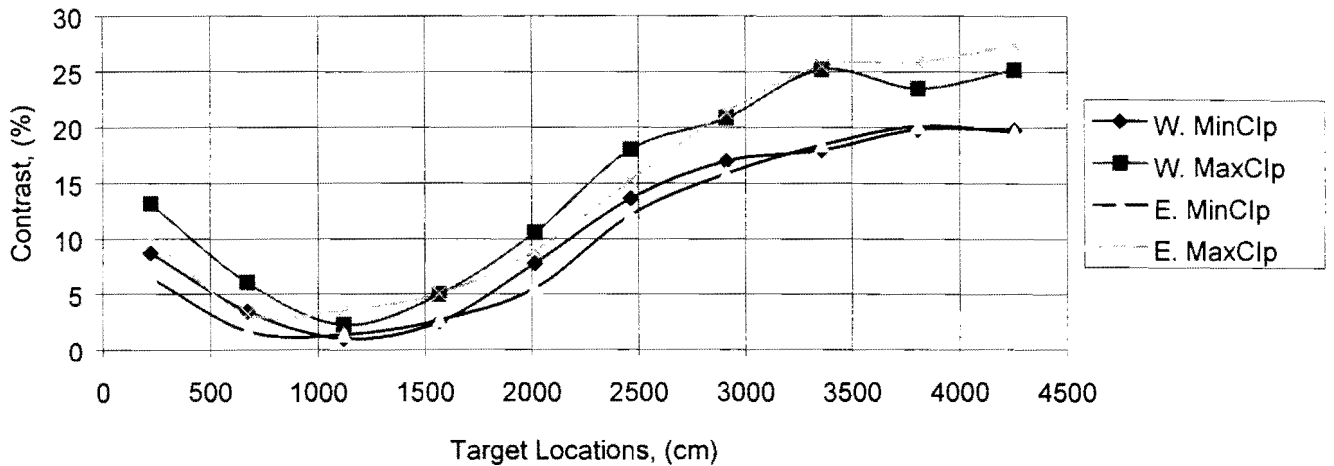


Figure 14 Contrast Between Poles 10A and 11A on the West and East Lines Under Original Conditions Using STV by Patching Method

The central limit theory was applied to obtain contrast distribution between illuminance assemblies mounted on poles 10A and 11A on the west and east lines. Again, contrast values of the target lie in the shaded areas with a 95% confidence level.

Analysis with Standard Fixture

All of the experiments were performed again after replacing the original heads with 250 Watt, General Electric luminaire heads. By applying the STV and STV with n points methods, contrast distributions were obtained between illuminance assemblies mounted on poles 9A and 10A as seen in Figures 15 and 16, respectively.

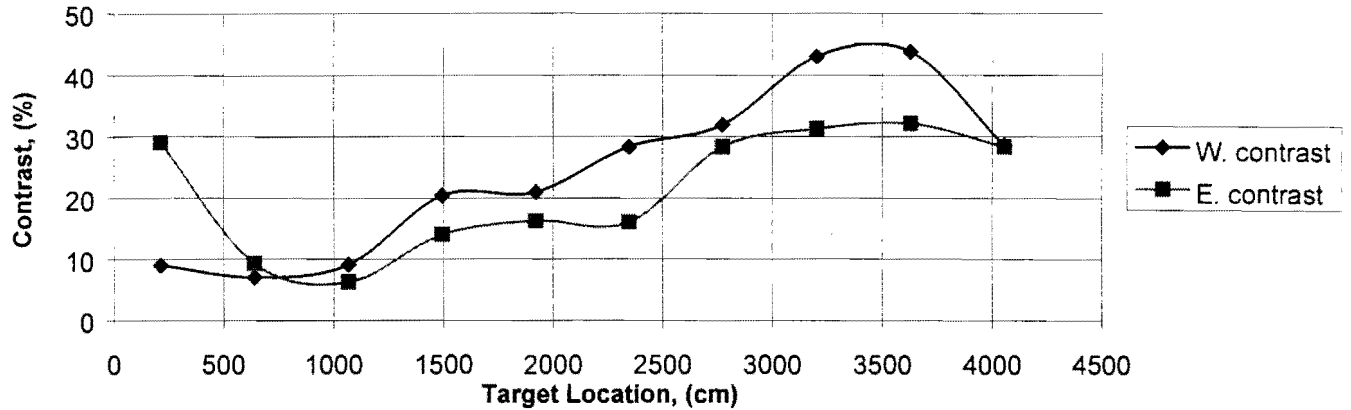


Figure 15 Contrast Between Poles 9A and 10A on the West and East Lines Under the Replaced 250 Watt Luminaire Heads Using STV Method

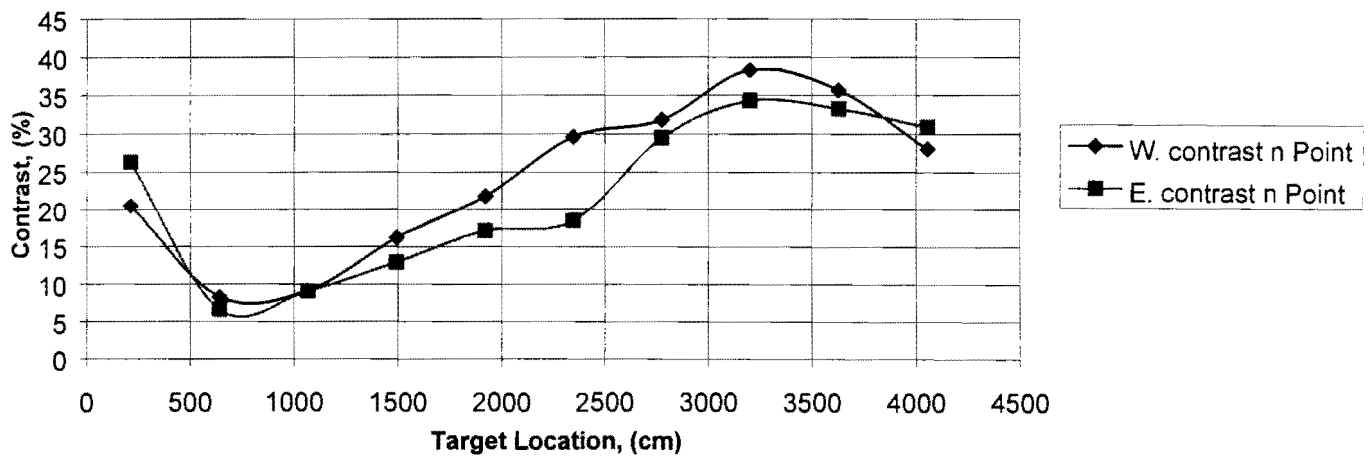


Figure 16 Contrast Between Poles 9A and 10A on the West and East Lines Under the Replaced 250 Watt Luminaire Heads Using STV with n Points Method

Figure 17 shows the difference between the STV and STV with n point methods for the west and east lines.

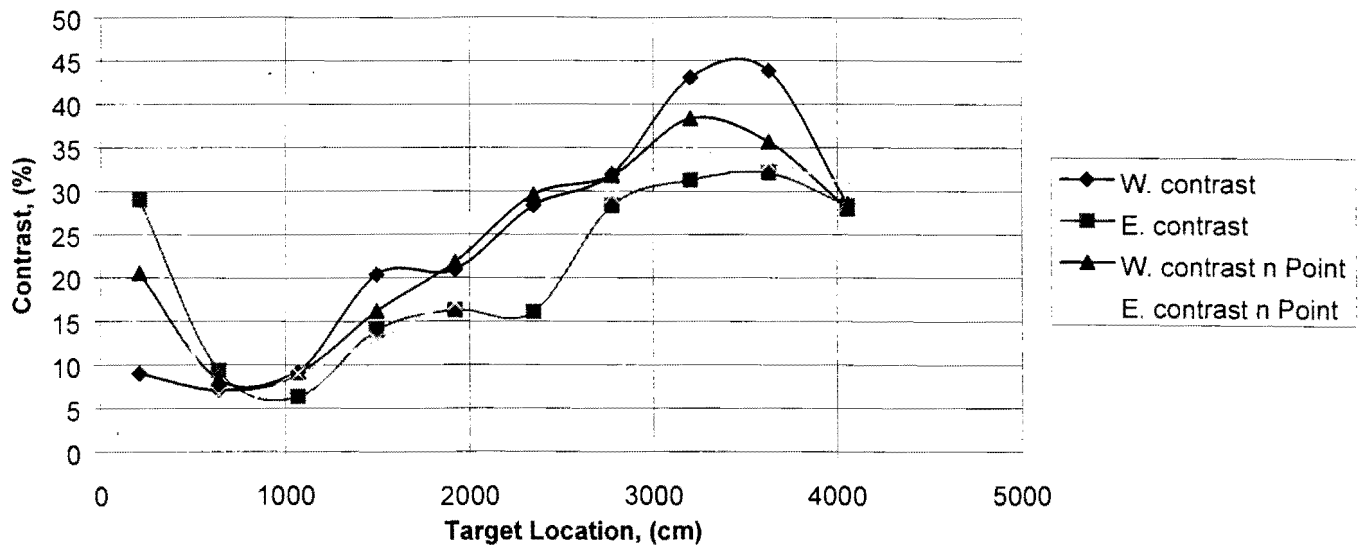


Figure 17 Contrast Comparison Between Poles 9A and 10A on the West and East Lines Under the Replaced 250 Watt Luminaire Heads Using STV and STV with n Points Methods

Figures 18 and 19 show contrast distribution between poles 9A and 10A using STV by comparing the areas and STV by patching methods using the central limit theory, respectively.

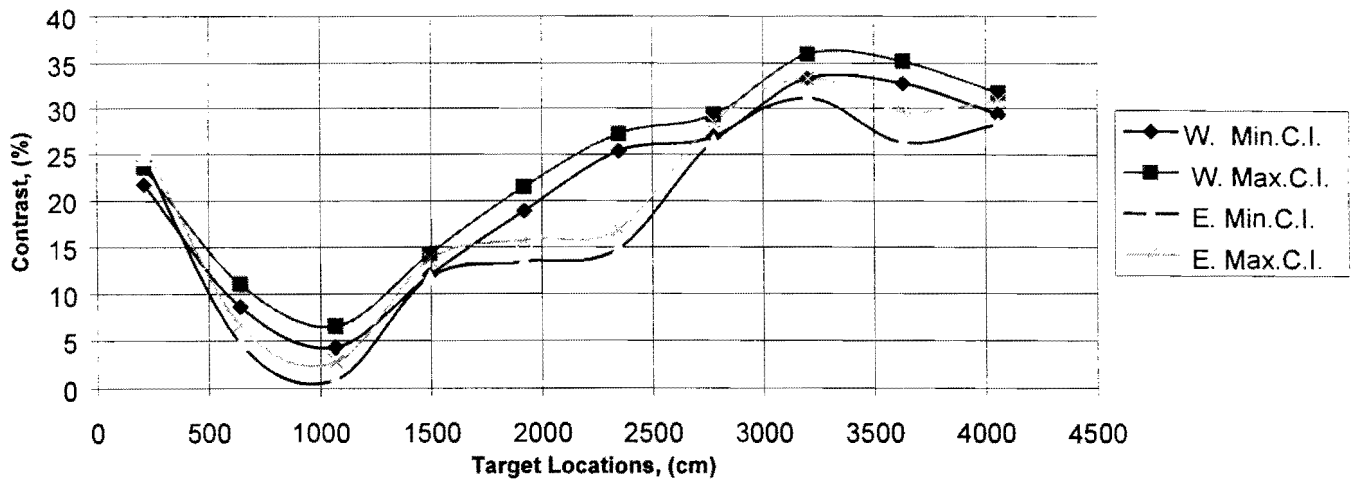


Figure 18 Contrast Between Poles 9A and 10A on the West and East Lines Under the Replaced 250 Watt Luminaire Heads Using STV by Comparing the Areas Method

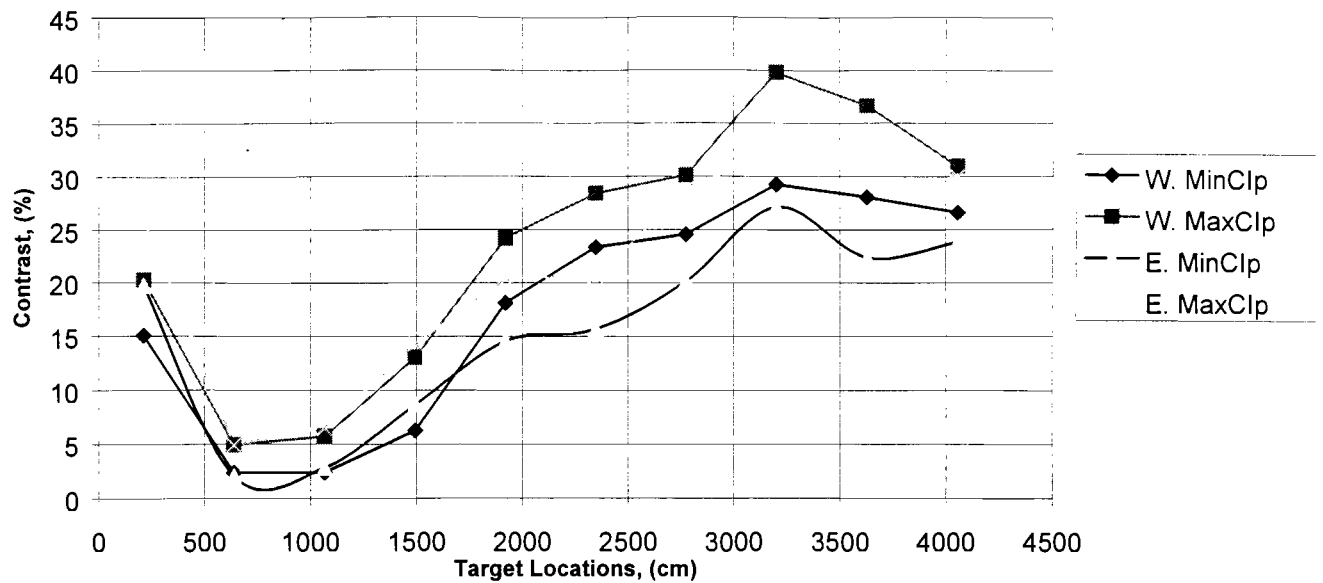


Figure 19 Contrast Between Poles 9A and 10A on the West and East Lines Under the Replaced 250 Watt Luminaire Heads Using STV by Patching Method

In Figures 20 and 21, contrast distributions were obtained between poles 10A and 11A by using the STV and STV with *n* point methods, respectively.

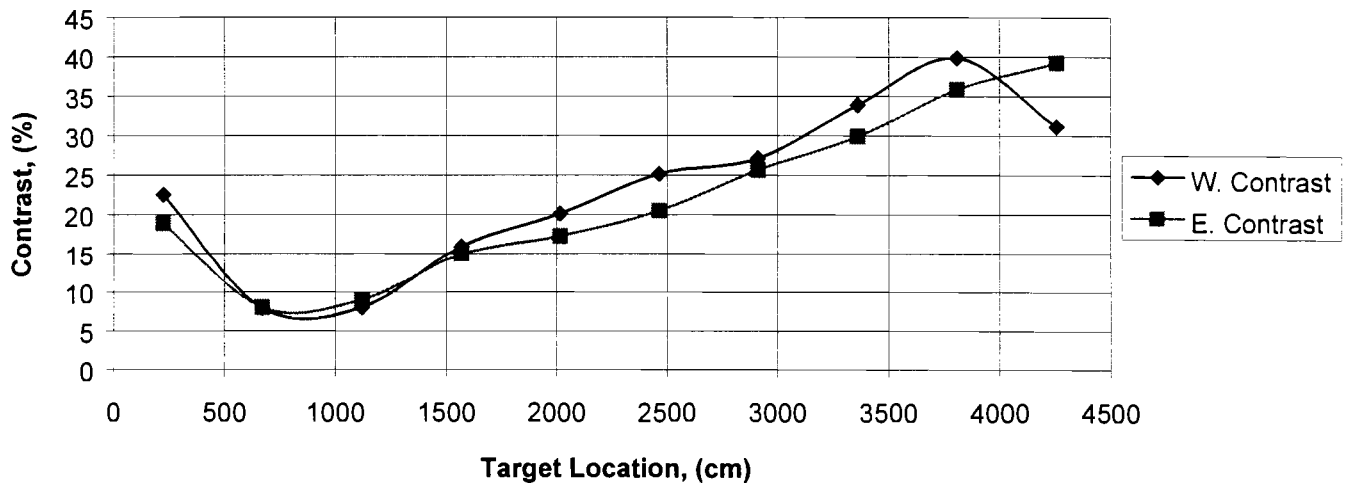


Figure 20 Contrast Between Poles 10A and 11A on the West and East Lines Under the Replaced 250 Watt Luminaire Heads Using STV Method

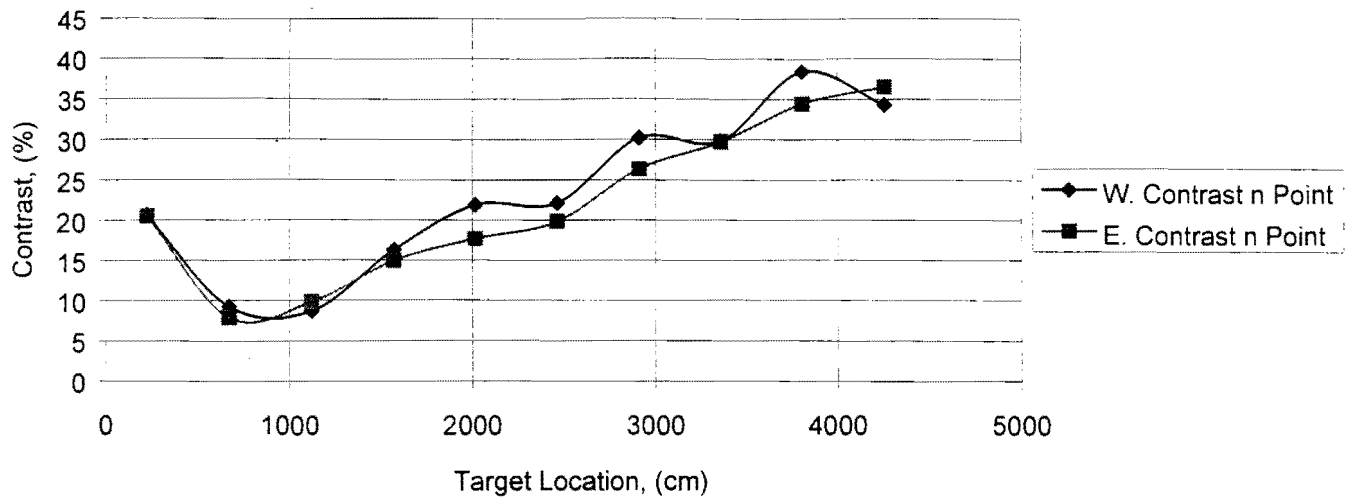


Figure 21 Contrast Between Poles 10A and 11A on the West and East Lines Under the Replaced 250 Watt Luminaire Heads Using STV with n Points Method

Figure 22 shows the difference between the STV and STV with n point methods for the west and east lanes.

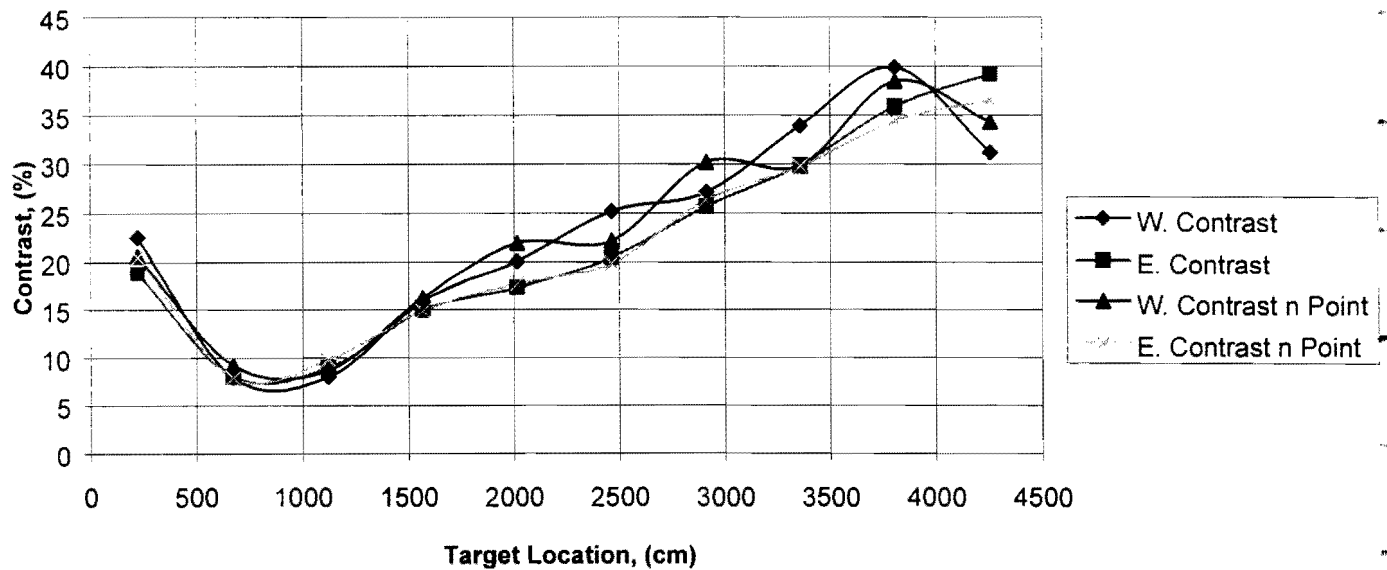


Figure 22 Contrast Comparison Between Poles 10A and 11A on the West and East Lines Under the Replaced 250 Watt Luminaire Heads Using STV and STV with n Points Methods

Figures 23 and 24 show contrast distribution between poles 10A and 11A for STV by comparing the areas and STV by patching methods using the central limit theory, respectively.

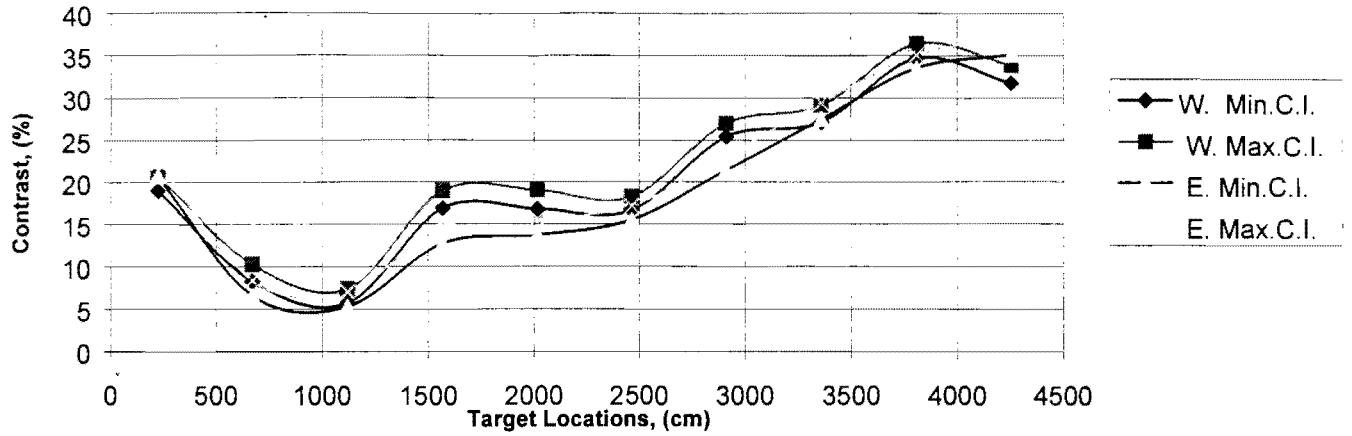


Figure 23 Contrast Between Poles 10A and 11A on the West and East Lines Under the Replaced 250 Watt Luminaire Heads Using STV by Comparing the Areas Method

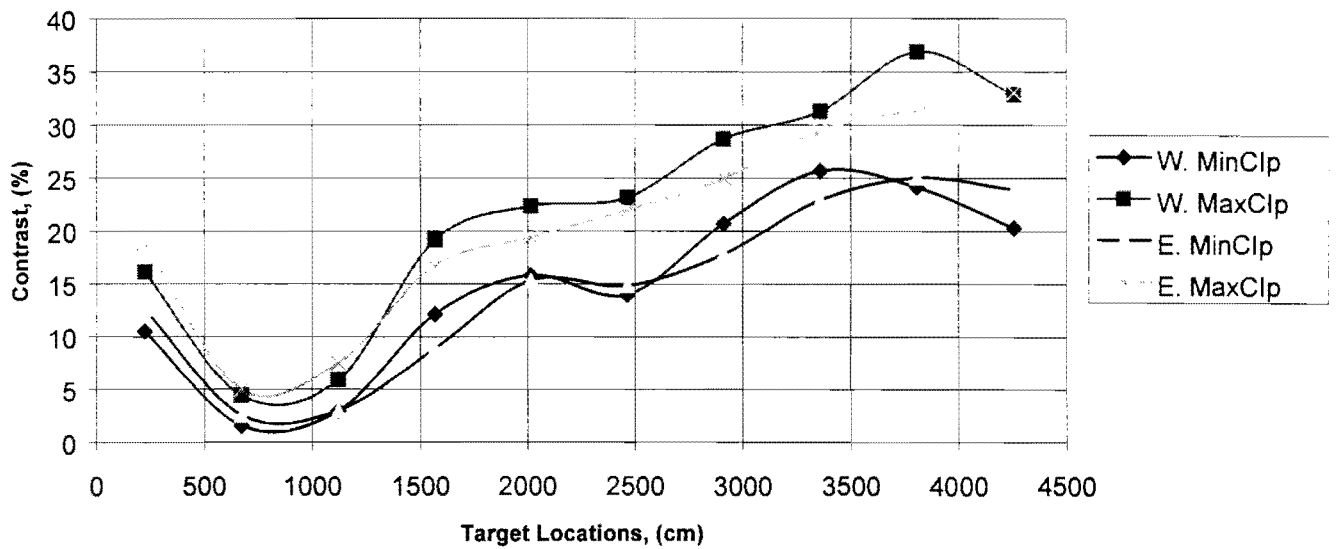


Figure 24 Contrast Between Poles 10A and 11A on the West and East Lines Under the Replaced 250 Watt Luminaire Heads Using STV by Patching Method

Figures 25 and 26 show contrast distribution using the STV, STV by taking n points, STV by comparing the areas, and STV by patching methods between illuminance assemblies mounted on poles 9A and 10A for the original conditions and after the 250 Watt luminaire heads were replaced, respectively.

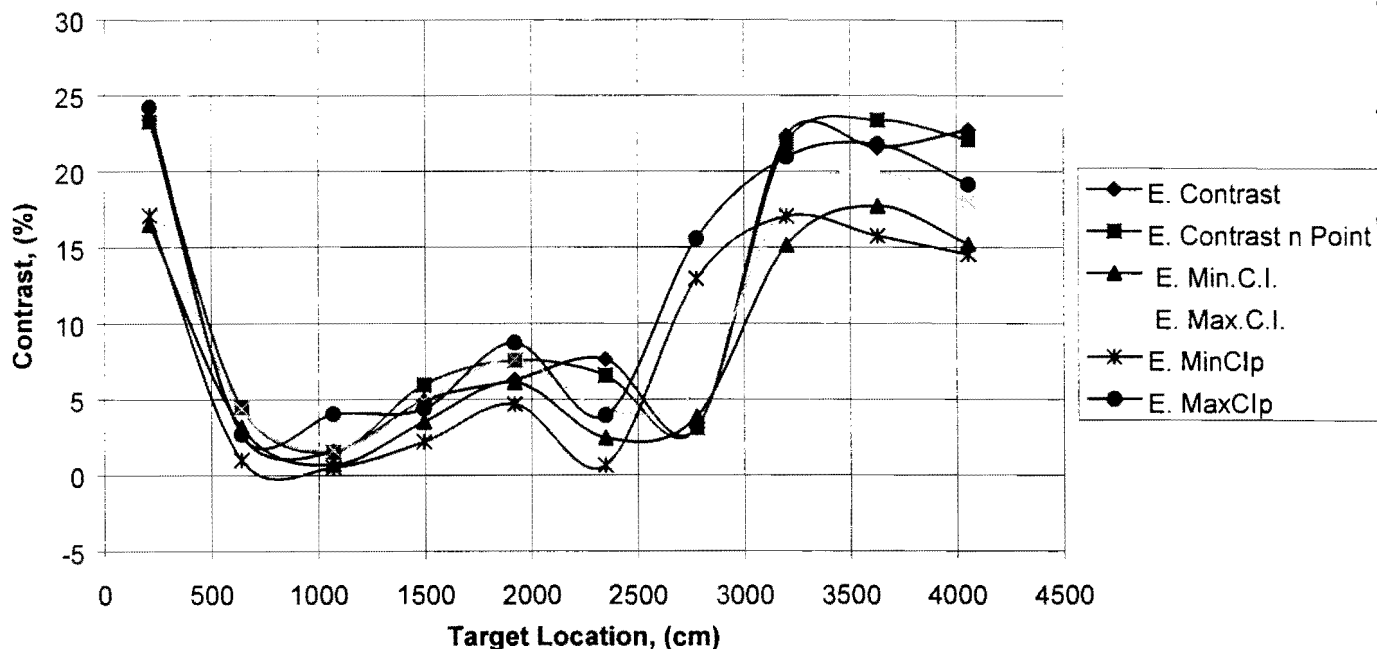


Figure 25 Contrast Comparison of STV, STV with n Points, STV by Comparing the Areas, and STV by Patching Methods Between Poles 9A and 10A on the East Line Under Original Conditions

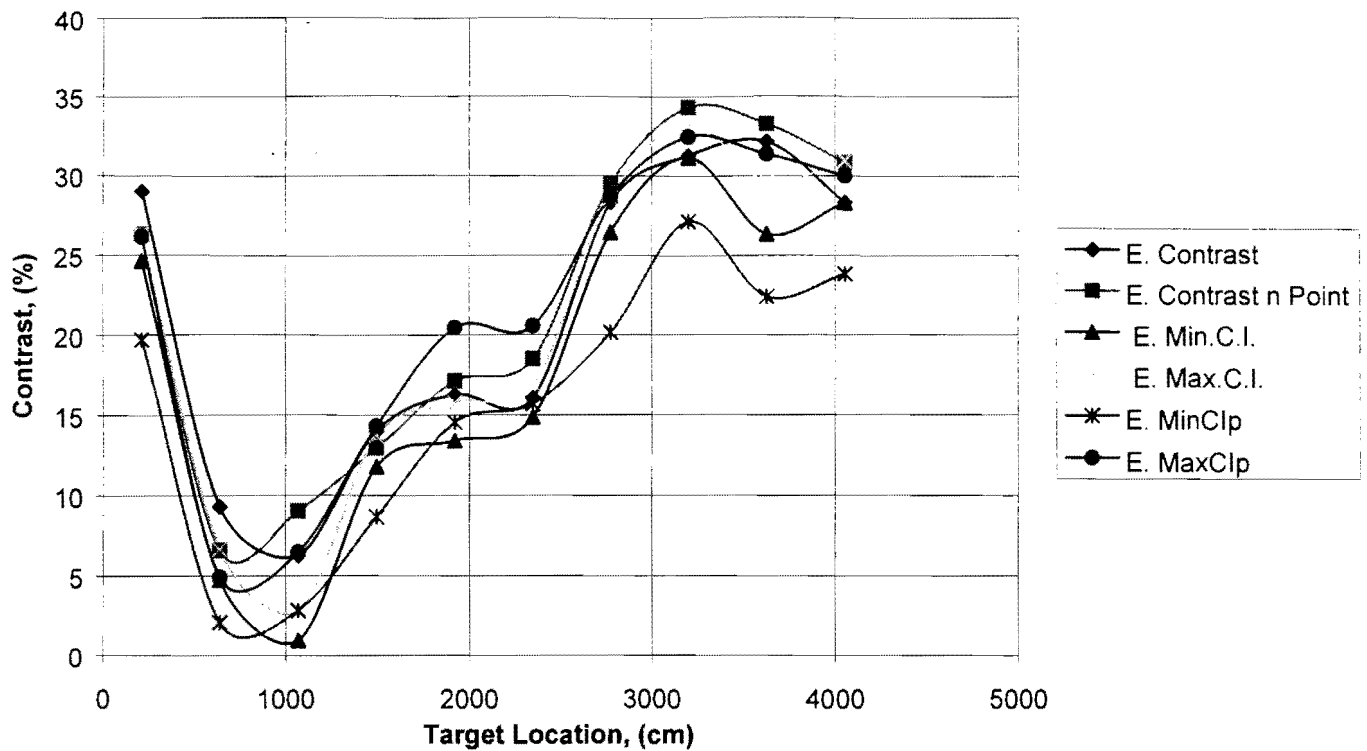


Figure 26 Contrast Comparison of STV, STV with n Points, STV by Comparing the Areas, and STV by Patching Methods Between Poles 9A and 10A on the East Line Under the Replaced 250 Watt Luminaire Heads

Figure 25 shows that the target was visible 40% of the distance between the luminaires mounted on poles 9A and 10A under the original conditions. Figure 26 shows that the target increased to 85% visible between the luminaires after the 250 Watt luminaire heads were replaced. Contrast distribution under the replaced luminaire heads became better than under the original conditions because the lamps were new and had clean lenses.

For experiments with the replaced 250 Watt luminaire heads, ten video camera images, in the order of the measurement locations, were plotted from pole 9A to 10A in the east lane. Figure 27 represents the video image at the first location. As shown in the figure, the target can be seen. Figures 28 and 29 show the video images at the 2nd and 3rd measurement locations, respectively. As shown in the figures, the target can not be seen at these locations. After the 3rd measurement location, target contrast gradually increases until pole 10A. Figures 30-36 represent target images at the 4th-10th target locations, respectively.

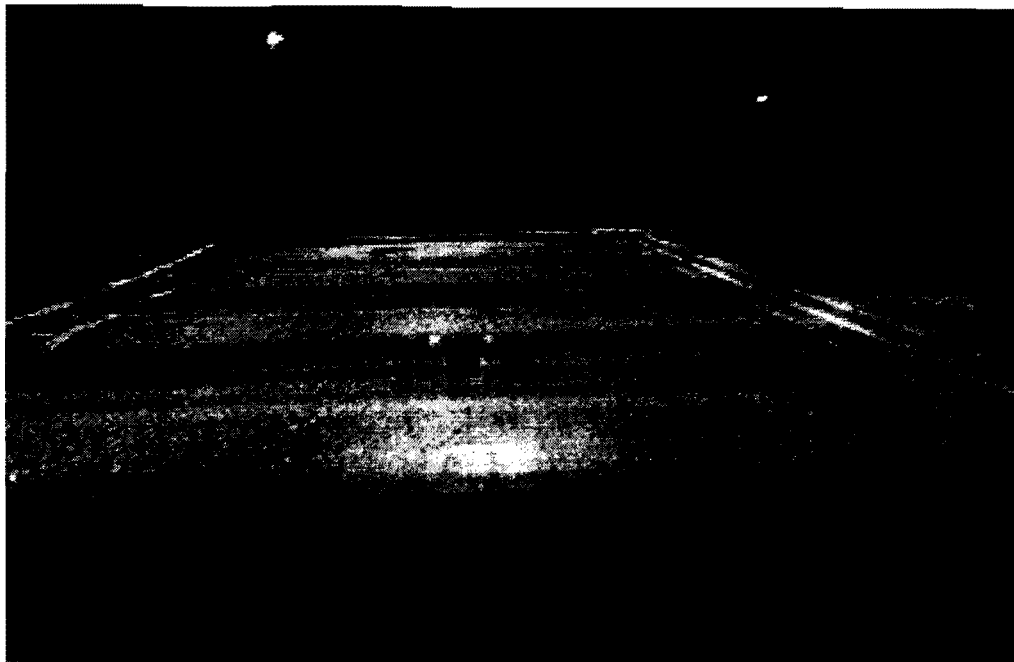


Figure 27 Video Image at the First Location



Figure 28 Video Image at the Second Location

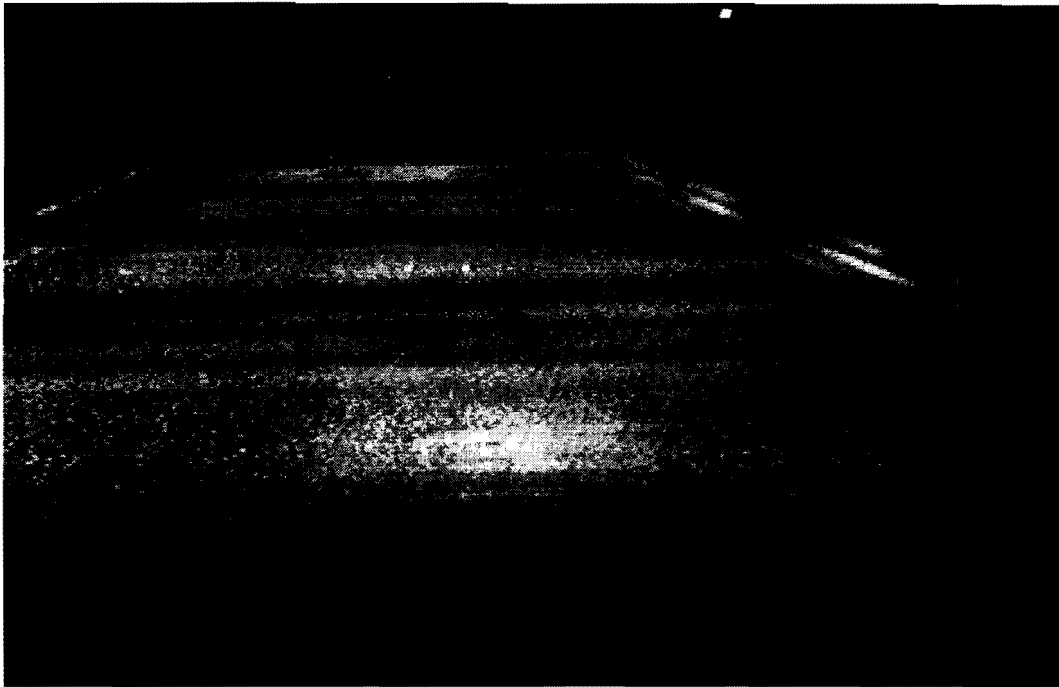


Figure 29 Video Image at the Third Location



Figure 30 Video Image at the Fourth Location

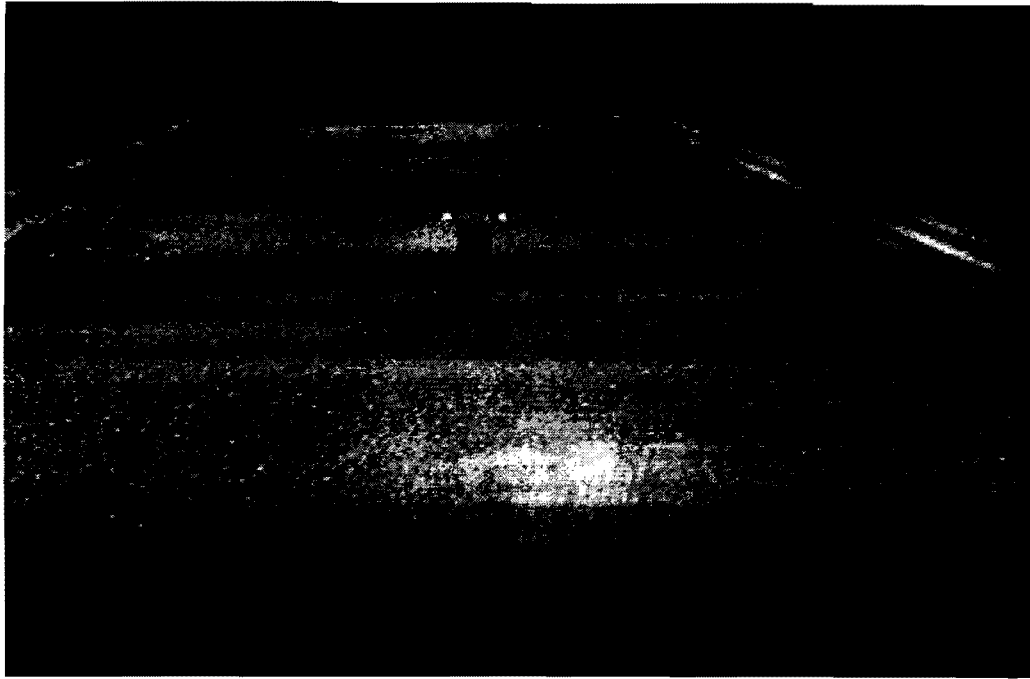


Figure 31 Video Image at the Fifth Location



Figure 32 Video Image at the Sixth Location

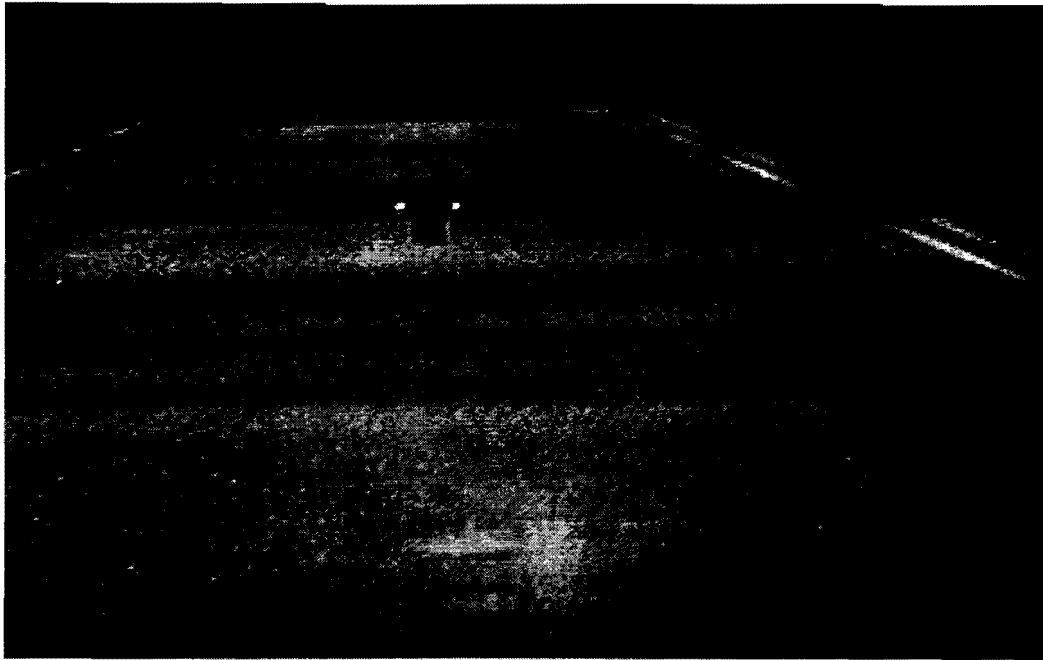


Figure 33 Video Image at the Seventh Location



Figure 34 Video Image at the Eighth Location

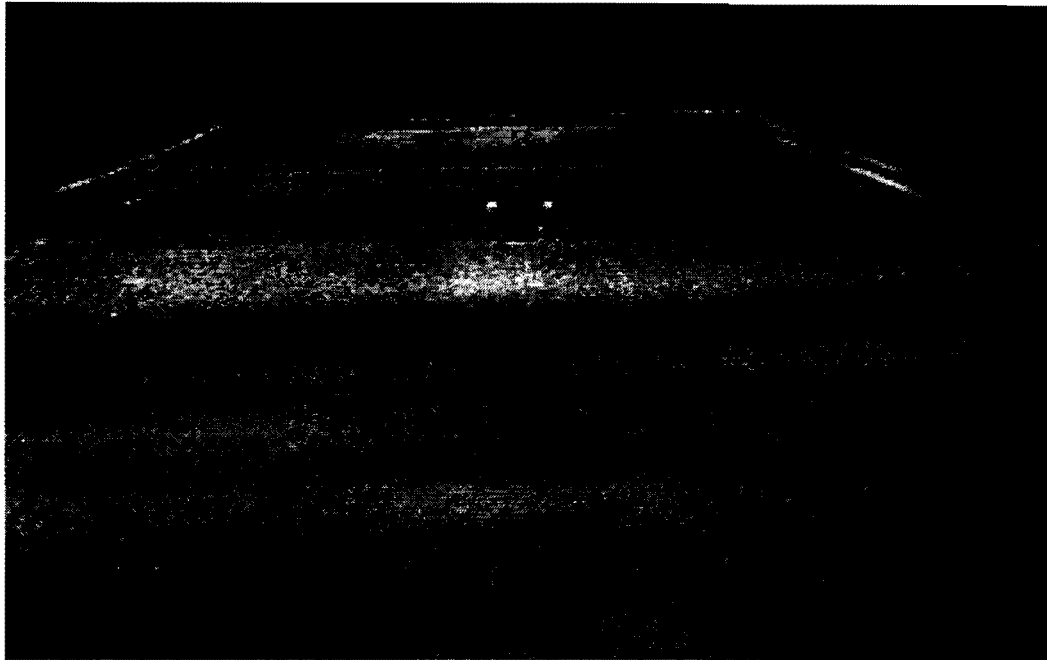


Figure 35 Video Image at the Ninth Location



Figure 36 Video Image at the Tenth Location

Conclusions

Experiments were performed between poles 9A and 10A and 10A and 11A under the original conditions and after replacing the original fixtures with the new 250 Watt luminaire heads. The same results were observed for the contrast distributions. The target had an 85% contrast between the illuminance assemblies mounted on the poles, but generally the target had no contrast at the 2nd and 3rd location.

The STV method is not a very reliable method to calculate the contrast of the targets since it just considers 5 idealized points at each target location, one point in the center of the target and four symmetrically placed points outside the boundaries of the target. In an idealized theory it may produce good results, but in practice the variations in luminous intensity across the surface of the pavement makes the potential for error very great. A larger sample of pavement

Experiment results show the target had a 40% contrast between illuminance assemblies mounted on poles 9A and 10A under the original conditions. Dirty lenses, old lamps, and mismatched wattages accounted for the low contrast, but after the new 250 Watt, G-E luminaire heads were replaced to the poles, the contrast increased to 85%. This demonstrates that non-linear dirt depreciation will have severe effect on STV.

Bibliography

Hall, R. R. and A. J. Fisher, (1978), "Measures of Visibility and Visual Performance in Road Lighting", Australian Road Research Board, Research Report No. 74.

Hayter, A. J. (1996), "Probability and Statistics for Engineer and Scientist", *PWS Publishing Company*, Boston.

Janoff, Micheal S., Loren K. Staplin and John B. Arens, (1986), "The Potential for Reduced Lighting on Roadways", *Public Road*, Vol. 50, No. 2, pp. 33 - 42.

Marsden, A. M. (1976), "Road Lighting - Visibility and Accident Reduction", *Journal of the Association of Public Lighting Engineers*, Vol. 41, No. 175, pp. 106 - 111.

Rackoff, Nick J. and Thomas H. Rackwell, (1975), "Driver Search and Scan Pattern in Night Driving", Ohio Department of Transportation and The Federal Highway Administration, Special Report 156.

Zwahlen, Helmut T. and Jing Yu, (1990), "Color and Shape Recognition of Reflectorized Targets under Automobile Low-Beam Illuminance at Night", *Transportation Research Record* 1327, pp. 1 - 7.

Sony Corporation, (1992), "CCD-VX3 Operation Manuel", 3-755-638-24 (1).